Supplemental Information

# Emulating Membrane Protein Environments – How Much Lipid is Required for a Native Structure: Influenza S31N M2

Anna K. Wright,[a,c†#] Joana Paulino,[a,c¶$] and Timothy A. Cross[a,b,c*]

[a]Institute of Molecular Biophysics, Florida State University, Tallahassee, Florida, 32306, United States

[b]Department of Chemistry and Biochemistry, Florida State University, Tallahassee, Florida, 32306, United States

[c]National High Magnetic Field Laboratory, Florida State University, Tallahassee, Florida, 32310, United States

*Email: timothyacross@gmail.com
Phone: 850-339-3186

## Supplementary Information

### Protein expression, purification, cleavage and reconstitution

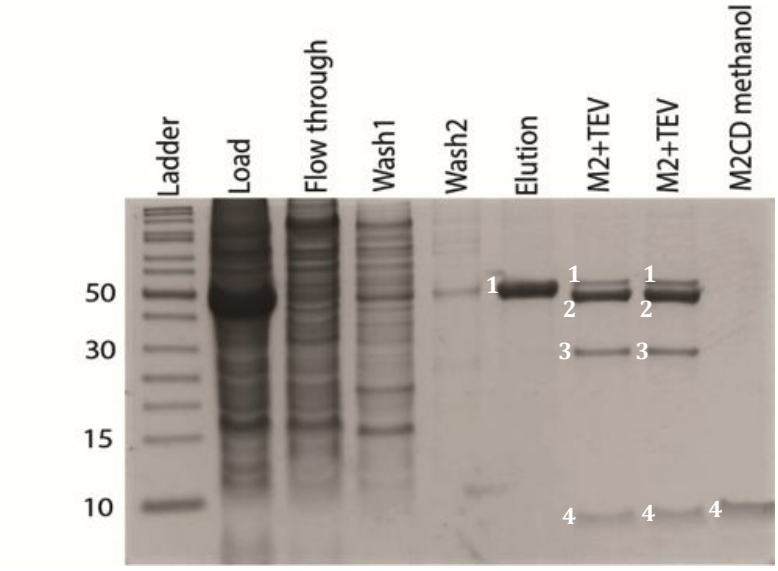


**Figure S1. S31N M2CD SDS-PAGE gel** demonstrating purification of M2-MBP fusion protein (protein band labeled with number (1), cleavage with Tobacco Etch Virus protease [1] – protein band labeled as number (2), and methanol extracted M2CD peptide (protein band labelled as number (4). After cleavage free MBP protein can be observed as indicated by protein band labelled as number (2). Ladder values of 50, 30, 15, and 10 are given in kDa.

### Solid State NMR spectroscopy

To measure anisotropic $^{15}N$ chemical shifts and $^{1}H$-$^{15}N$ dipolar couplings using either the SAMPI4[2] or PISEMA[3, 4] pulse sequence the data were acquired at 720 MHz, utilizing a low-E $^{1}H/^{15}N$ double resonance probe. Acquisition took place at 303K, above the gel to liquid crystalline phase transition temperature of DOPC/DOPE lipids. Experimental parameters included a 90° pulse of 5ms and cross-polarization contact time of 0.9 ms, 4 s recycle delay and SPINAL decoupling sequence[5]. 22-28 $t_1$ points were acquired with 2048 transients. Spectral processing was done with NMRPIPE[6] and plotting with SPARKY. $^{15}N$ chemical shifts were referenced to a concentrated solution of $N_2H_8SO_4$, defined as 26.8 ppm relative to liquid ammonia. MAS experiments included previously mentioned REDOR, NCA and DARR pulse sequences. All were performed at 600MHz, utilizing a low-E triple resonance probe, in a $^{1}H$-$^{13}C$-$^{15}N$ or $^{1}H$-$^{13}C$-$^{2}H$ configuration.

### Structural Analysis

The $\phi/\psi$ torsion angles measured from the 2L0J Wild Type and 2N70 S31N mutant structures are presented in **Table S1** along with the Magic Angle Spinning $^{13}Ca$ ssNMR frequencies. For the 2L0J structures these frequencies were observed and published by Can et al., (2012)[7]. These values in Table S1 are compared with the observed values from Andreas et al., (2015)[8]. In addition, for both of these Ca data sets we present the TALOS predicted backbone torsion angles. The 2L0J structure which is largely based on Oriented Sample ssNMR restraints has a very well-defined backbone structure. The 2N70 structure based on distance restraints is less well-defined having more scatter in the $\phi/\psi$ torsion angle than is typical of transmembrane helices[9, 10]. The

2N70 chemical shifts for the non-primed pair of helices have two sites (I32 & I39) displaying atypical chemical shifts for helical residues facing a lipid environment. Data for the primed helix of 2N70 is only available from D26-L43. A comparison of the chemical shifts excluding S/N31for the primed helix (S31N M2CD) and the data from Can et al., (WT M2CD) generates an rmsd of just 0.45 ppm and if Val28 is excluded it is a mere 0.29 ppm. Absolutely remarkable agreement. However, such a comparison for the non-prime helix results in an rmsd of 1.86 ppm and even without I32 and I39 the rmsd is 0.88 ppm approximately double the rmsd of the primed helix. Clearly the non-prime helix is distorted not just at the I32 and I39 sites but throughout the helix.

For these three sets of Ca chemical shifts we present the TALOS predicted backbone torsion angles. The I32 and I39 residues on the presumed lipid facing surface of the structure should have nearly ideal TM helical torsion angles ($\phi$=-60°, $\psi$=-45°) instead they have significantly distorted torsion angles for a transmembrane helical structure. The average $\phi/\psi$ values for L26-L43 for 2L0J is -61.1±3.0°/-43.4±3.1° very close to the typical value for TM helices in the environment where the helical hydrogen bonds are strengthened. The 2N70 structure is a dimer of dimer structure and consequently two averages were achieved, one for the primed helices (-63.4°±9.5°-45.6°±10.0°) and one for the non-primed pair of helices (-61.1°±6.6°/-41.4°±6.5°). The variations in the torsion angles are especially large in the primed helices and atypical of the uniform helical structure observed in most TM helices in contact with the lipid bilayer.

**Table S1: Ca frequencies of WT and S31N M2 and their analysis with TALOS**

| **AA** | **2L0J (WT)** | | | **2N70 (S31N)** | | |
|---|---|---|---|---|---|---|
| | $\phi/\psi$ | $^{13}$Ca $\nu_{iso}$ (ppm) | TALOS $\phi/\psi$ | $\phi/\psi$ | $^{13}$Ca $\nu_{iso}$ (ppm) | TALOS $\phi/\psi$ |
| L26 | -63.5/-50 | 58.2 | -64/-38 | -61/-47.6 | 58.1 | -62/-37 |
| L26’ | | | | -73.0/-45.6 | 57.9 | -63/-37 |
| V27 | -66.9/-40.9 | 67.2 | -62/-43 | -62.6/-33.6 | 66.1 | -66/-46 |
| V27’ | | | | -60.3/-56.0 | 66.6 | -66/-45 |
| V28 | -61.4/-48.9 | 67.1 | -63/-42 | -66.3/-59.9 | 66.7 | -61/-47 |
| V28’ | | | | -59.9/-54.4 | 65.6 | -61/-41 |
| A29 | -60.3/-44.7 | 55.8 | -58/40 | -47.7/-39.4 | 55.2 | -61/-39 |
| A29’ | | | | -54.0/-24.3 | 55.4 | -62/-43 |
| A30 | -61.1/-40.3 | 55.3 | -65/-41 | -71.3/-32.0 | 55.0 | -67/-35 |
| A30’ | | | | -89.0/-20.7 | 55.4 | -63/-37 |
| S/N31 | -66.3/-51.2 | 63.2 | -66/-43 | -67.2/-63.2 | 54.7 | -78/-35 |
| S/N31’ | | | | -74.9/-42.0 | 58.0 | -65/-42 |
| I32 | -49.3/-45.4 | 65.8 | -63/-42 | **-50.9/-38.5** | **61.4** | **-104/-9** |

| | | | | | | |
|---|---|---|---|---|---|---|
| I32’ | | | | -51.9/-42.9 | 65.6 | -61/-42 |
| I33 | -59.0/-37.0 | 65.8 | -62/-44 | -54.9/-44.2 | 64.3 | -78/-30 |
| 133’ | | | | -75.9/-34.7 | 66.0 | -62/-43 |
| G34 | -61.3/-39.5 | 48.2 | -64/-44 | -55.5/-48.4 | 47.6 | -59/-43 |
| G34’ | | | | -59.1/-44.5 | 47.9 | -63/-42 |
| I35 | -64.2/-45.7 | 65.7 | -63/-41 | -70.5/-38.3 | 64.1 | -67/-45 |
| 135’ | | | | -66.6/-57.3 | 66.1 | -63/-41 |
| L36 | -55.3/-43.8 | 58.3 | -61/-41 | -69.2/-35.9 | 57.6 | -61/-35 |
| L36’ | | | | -49.4/-36.9 | 58.1 | -61/-41 |
| H37 | -62.9/-42.3 | 59.5 | -63/-42 | -55.7/-48.0 | 59.3 | -62/-46 |
| H37’ | | 62.4 | | -57.3/-57.3 | 62.3 | -64/-40 |
| L38 | -62.0/-41.6 | 58.4 | -61/-40 | -67.8/-37.0 | 58.4 | -67/-34 |
| L38’ | | | | -51.7/-50.4 | 58.3 | -65/-42 |
| I39 | -62/-40.8 | 65.7 | -64/-43 | **-49.8/-39.1** | **60.4** | **-90/-13** |
| I39’ | | | | -53.0/-32.0 | 65.5 | -62/-46 |
| L40 | -61.4/-40.8 | 58.2 | -59/-42 | -73.7/-35.1 | 58.5 | -62/-41 |
| L40’ | | | | -82.3/-59.1 | 58.1 | -63/-37 |
| W41 | -63.3/-39.9 | 61.4 | -66/-41 | -60.7/-56.6 | 60.7 | -62/-42 |
| W41’ | | 63.2 | | -49.8/-42.8 | 62.6 | -67/-41 |
| I42 | -65.4/-46.2 | 65.8 | -62/-44 | -55.3/-41.1 | 64.2 | -64/-44 |
| I42’ | | | | -72.7/-42.0 | 65.8 | -61/-45 |
| L43 | -53.8/-43.0 | 58.2 | -61/-40 | -60.7/-36.9 | 57.7 | -64/-40 |
| L43’ | | | | -59.8/-28.5 | 58.1 | -67/-39 |

**Sample Preparation:**

$^{15}$N labeled V28, A30 and Ile42 M2 TMD (22-46) and $^{13}$C,$^{15}$N-labeled V27,A30,N31,G34 were synthesized using Fmoc (9-fluorenylmethoxycarbonyl) chemistry. Fmoc-[15N]-Val, Fmoc-[15N]-Ala, Fmoc-[$^{15}$N]-Ile, Fmoc-[$^{13}$C,$^{15}$N]-Asn, Fmoc –[$^{13}$C,$^{15}$N]-Gly, were purchased from Cambridge Isotope Laboratory (Andover, MA). Solid-phase 0.25 mmol syntheses of M2 TMP were performed on an Applied Biosystems 430A peptide synthesizer as previously described. The peptide was cleaved from the resin by the treatment with ice cold 95% TFA, 2.5% H2O, 1.25% ethanedithiol, 1.25% thioanisole

and precipitated from TFA using ice cold ether. Following centrifugation, the supernatant was discarded and the pellet was washed with cold ether again. The precipitated peptide was dried under vacuum. Peptide purity and identity was confirmed using ESI mass spectrometry (positive ion mode).

$^{15}$N-$V_{28}A_{30}I_{42}$ S31N M2 TM was co-dissolved in trifluoroethanol (TFE) with DMPC in a 1:30 molar ratio. The solvent was removed under a stream of nitrogen gas to yield a lipid film, and then dried to remove residual organic solvent under vacuum for 12 hours. Thoroughly dried lipid film was hydrated with 8mL of 10mM HEPES buffer at pH 7.5 to form multilamellar vesicles containing M2 TMP in tetrameric state. This suspension was bath sonicated, dialyzed against 2L HEPES 10mM pH 7.5 buffer for 1 day and centrifuged at 196,000xg to harvest unilamellar proteoliposomes.

*NMR Spectroscopy*

There were no indications of resonance doubling even for N31 in the spectroscopy of the S31N M2TM (residues 22-46). The $^{15}$N and $^{13}$Ca chemical shifts for selected sites from MAS ssNMR spectra are presented in **Table S2**.

Furthermore, the RMSD between the prime helix of Andreas et al., and Can et al., 2012 excluding the mutated site (31) is just 0.45 ppm and if the data for residue 28 is removed the RMSD drops to 0.29 ppm. This remarkable agreement confirms the excellent characterization of the primed helix and further suggests that it is the non-prime helix that is breaking the four fold symmetry of the 2N70 structure.

**Table S2: Isotropic chemical shifts obtained from NCA spectra of $V_{27}A_{30}N_{31}G_{34}$ S31N M2TM** in DMPC lipid bilayers at pH 7.5 compared to 2N70 chemical shifts

| | S31N M2TM | | 2N70 Non-Primed | | 2N70 Primed | |
|---|---|---|---|---|---|---|
| AA | $^{15}$N (ppm) | $^{13}$Ca (ppm) | $^{15}$N (ppm) | $^{13}$Ca (ppm) | $^{15}$N (ppm) | $^{13}$Ca (ppm) |
| V27 | 122.3 | 66.3 | 119.3 | 66.1 | 119.1 | 66.6 |
| A30 | 119.3 | 55.8 | 118.9 | 55.0 | 117.9 | 55.4 |
| N31 | 115.5 | 57.6 | 110.8 | 54.7 | 115.6 | 58.0 |
| G34 | 107.7 | 48.0 | 109.8 | 47.6 | 106.8 | 47.9 |

**Table S3: Observed and** Predicted **$^{15}$N Anisotropic Chemical Shift and $^{1}$H-$^{15}$N Dipolar Couplings for the S31N M2CD** in DOPC/DOPE at pH 7.5.

Presented in Table S3 are the anisotropic $^{15}$N chemical shifts (ACS) [4] and $^{1}$H-$^{15}$N dipolar couplings (DC) observed from S31N M2CD. Sample preparation was as described in the main text. Out of the 12 observed anisotropic chemical shift [4] interactions only 3 ACS observations were consistent (±10 ppm) with the non-primed helix predictions and only 3 ACS values were consistent with the primed helix predictions of 2N70. For the anisotropic dipolar coupling (DC) observations 6 were consistent (± 1kHz) with the nonprimed helix and only 3 were consistent with the primed helix. Note the dramatic differences between the predicted values for the primed helix and non-primed helix. For oriented sample ssNMR spectroscopy, after ultracentrifugation the pellet was resuspended in 5mM Tris HCl pH 7.5 buffer to a final volume of 1200µl and deposited onto glass

slides, with 30µL of the proteoliposome suspension applied to each 5.7mm x 12 mm surface of the 60µm thick slides (total 40 slides).

| | **Observed** | | **Predicted from Structures** | |
|---|---|---|---|---|
| Residue | DC (kHz) | ACS (ppm) | 2N70 | 2N70' |
| L26 | | | 4.8/212.4 | 2.4/191.4 |
| V27 | **7.9** | **163.9** | **8.4/191.3** | **8.3/156.0** |
| V28 | **4.5** | **135.8** | **5.0/141.9** | **7.9/199.3** |
| A29 | | | 4.8/201.9 | 6.1/180.9 |
| A30 | | | 6.3/213.2 | 3.5/201.9 |
| N31 | | | 7.7/148.0 | 10.2/199.3 |
| I32 | **3.4** | **150.3** | **7.3/185.3** | **7.2/171.9** |
| I33 | **2.4** | **192.2** | **4.3/207.7** | **3.2/197.4** |
| G34 | | | 8.0/200.4 | 9.5/211.4 |
| I35 | **5.6** | **136.7** | **8.6/167.6** | **9.0/181.9** |
| L36 | **4.3** | **159.3** | **3.8/184.5** | **8.5/212.9** |
| H37 | | | 7.1/224.3 | 7.4/225.3 |
| L38 | **7.3** | **169.9** | **9.7/204.4** | **8.6/205.7** |
| I39 | **4.9** | **145.1** | **6.9/162.2** | **9.7/189.2** |
| L40 | **1.7** | **184.9** | **2.4/189.1** | **4.2/191.5** |
| W41 | | | 8.9/209.3 | 8.0/219.6 |
| **I42** | **9.4** | **163.3** | **9.3/174.6** | **10.2/200.7** |
| **L43** | **5.0** | **155.7** | **5.0/172.3** | **7.6/184.1** |
| D44 | | | 4.0/206.2 | 4.2/200.4 |
| R45 | | | 7.4/192.4 | 8.7/216.9 |
| **L46** | **6.7** | **137.2** | **4.7/134.8** | **8.9/184.5** |
| **I51** | **4.3** | **74.4** | | |
| **L59** | **3.5** | **87.8** | | |

References:


1. Stouffer, A.L., et al., *Structural basis for the function and inhibition of an influenza virus proton channel.* Nature, 2008. **451**(7178): p. 596-599.
2. Nevzorov, A.A. and S.J. Opella, *A "magic sandwich" pulse sequence with reduced offset dependence for high-resolution separated local field spectroscopy.* J Magn Reson, 2003. **164**(1): p. 182-6.

3. Wu, C.H., A. Ramamoorthy, and S.J. Opella, *High-Resolution Heteronuclear Dipolar Solid-State NMR Spectroscopy.* Journal of Magnetic Resonance, Series A, 1994. **109**(2): p. 270-272.
4. Kovacs, F.A. and T.A. Cross, *Transmembrane four-helix bundle of influenza A M2 protein channel: structural implications from helix tilt and orientation.* Biophys J, 1997. **73**(5): p. 2511-7.
5. Fung, B.M., A.K. Khitrin, and K. Ermolaev, *An Improved Broadband Decoupling Sequence for Liquid Crystals and Solids.* Journal of Magnetic Resonance, 2000. **142**(1): p. 97-101.
6. Delaglio, F., et al., *NMRPipe: a multidimensional spectral processing system based on UNIX pipes.* J Biomol NMR, 1995. **6**(3): p. 277-93.
7. Can, T.V., et al., *Magic angle spinning and oriented sample solid-state NMR structural restraints combine for influenza A M2 protein functional insights.* Journal of the American Chemical Society, 2012. **134**(22): p. 9022-9025.
8. Andreas, L.B., et al., *Structure and mechanism of the influenza A M218–60 dimer of dimers.* Journal of the American Chemical Society, 2015. **137**(47): p. 14877-14886.
9. Kim, S. and T.A. Cross, *Uniformity, ideality, and hydrogen bonds in transmembrane α-helices.* Biophysical Journal, 2002. **83**(4): p. 2084-2095.
10. Page, R.C., S. Kim, and T.A. Cross, *Transmembrane helix uniformity examined by spectral mapping of torsion angles.* Structure, 2008. **16**(5): p. 787-797.